Supplementary
Plant phenology evaluation of CRESCENDO land surface models. Part I: onset and offset timings.

Daniele Peano[1], Deborah Hemming[2], Stefano Materia[1], Christine Delire[3], Yuanchao Fan[4,5], Emilie Joetzjer[3], Hanna Lee[4], Julia E.M.S. Nabel[6], Taejin Park[7,8], Philippe Peylin[9], David Wårlind[10], Andy Wiltshire[2,11], and Sönke Zaehle[12]

[1]Fondazione Centro Euro-Mediterraneo sui Cambiamenti Climatici, CSP, Bologna, Italy
[2]Met Office Hadley Centre, Exeter, UK
[3]Centre National de Recherches Météorologiques, UMR3589, Université de Toulouse/Météo-France/CNRS, Toulouse, France
[4]NORCE Norwegian Research Centre AS, Bergen, Norway
[5]Harvard University, Cambridge, USA
[6]Max Planck Institute for Meteorology, Hamburg, Germany
[7]NASA Ames Research Centre, CA, USA
[8]Bay Area Environmental Research Institute, CA, USA
[9]Laboratoire des Sciences du Climat et l'Environnement, Gif-sur-Yvette, France
[10]Department of Physical Geography and Ecosystem Science, Faculty of Science, Lund University, Sweden
[11]Global Systemss Insitute,University of Exeter, Exeter, UK
[12]Max Planck Institute for Biogeochemistry, Jena, Germany

Correspondence: Daniele Peano (daniele.peano@cmcc.it)

This document contains:

- Supplementary Figure 1 displays a schematic representation of the Four-Growing-Season Type method;
- Supplementary Figure 2 contains the distribution of the four growing season types for the three satellite products;
- Supplementary Figure 3 contains the distribution of the agreement regions for the four growing season types between Land Surface Models (LSM) and LAI3g;
- Supplementary Table 1 contains the percentage of agreement for each growing season type between LAI3g and LSM;
- Supplementary Figure 4 contains the distribution of the agreement regions for the four growing season types between Land Surface Models (LSM) and SENTINEL;
- Supplementary Table 2 contains the percentage of agreement for each growing season type between SENTINEL and LSM;
- Supplementary Figure 5 contains the global climatological growing season start and end timings for LAI3g and SENTINEL;

- Supplementary Figure 6 contains the differences in growing season start timings between LAI3g and each Land Surface Model;
- Supplementary Figure 7 contains the differences in growing season end timings between LAI3g and each Land Surface Model;
- Supplementary Table 3 contains the fraction of land grid-cell in agreement with LAI3g for each land surface model in Onset and Offset timings;
- Supplementary Table 4 contains the average difference between LAI3g and MODIS, SENTINEL, each land surface model, and multi-model ensemble mean (MME) in Growing Season Start (GSS) and Growing Season End (GSE) timings;
- Supplementary Figure 8 contains the differences in growing season start timings between SENTINEL and each Land Surface Model;
- Supplementary Figure 9 contains the differences in growing season end timings between SENTINEL and each Land Surface Model;
- Supplementary Table 5 contains the fraction of land grid-cell in agreement with SENTINEL for each land surface model in Onset and Offset timings;
- Supplementary Table 6 contains the average difference between SENTINEL and LAI3g, MODIS, each land surface model, and multi-model ensemble mean (MME) in Growing Season Start (GSS) and Growing Season End (GSE) timings;
- Supplementary Figure 10 contains the zonal mean of growing season start and end timings in three specific subregions: Americas; Europe plus Africa; Asia plus Oceania;
- Supplementary Figure 11 contains the distribution of the four growing season types of each Land Surface Model (LSMs) and MODIS.

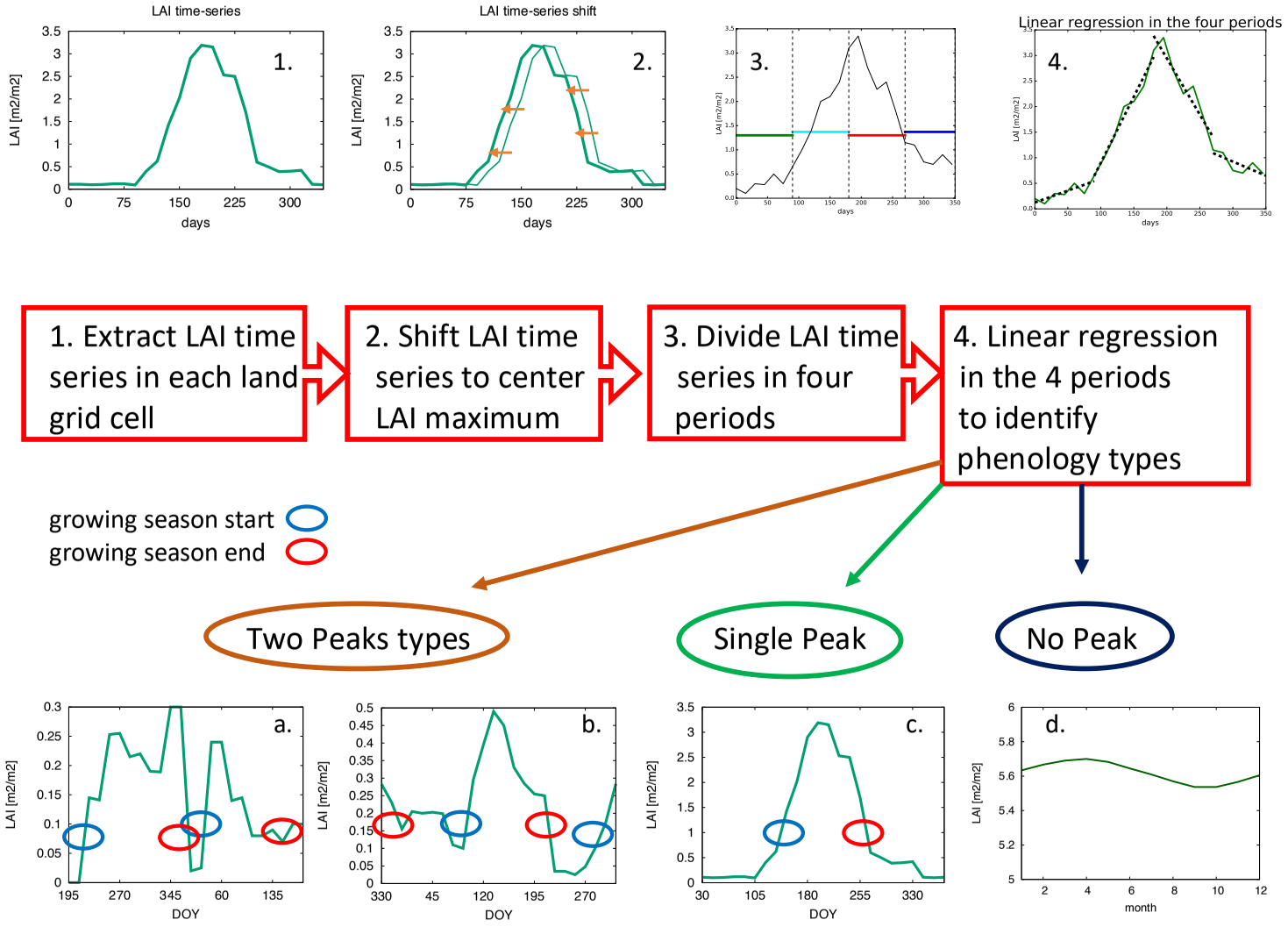

Supplementary Figure 1. Scheme of the Four-Growing-Season Type method used in evaluating onset and offset of the growing season. The evergreen type (panel d) is identified based on relative changes in LAI compared to local LAI mean value. The other three types, namely single growing season peaking in summer, single growing season with summer dormancy, and two growing season, are identified based on LAI annual cycle shapes, LAI slopes and transition timings, and critical threshold. Further details can be found in *Peano et al.* (2019)

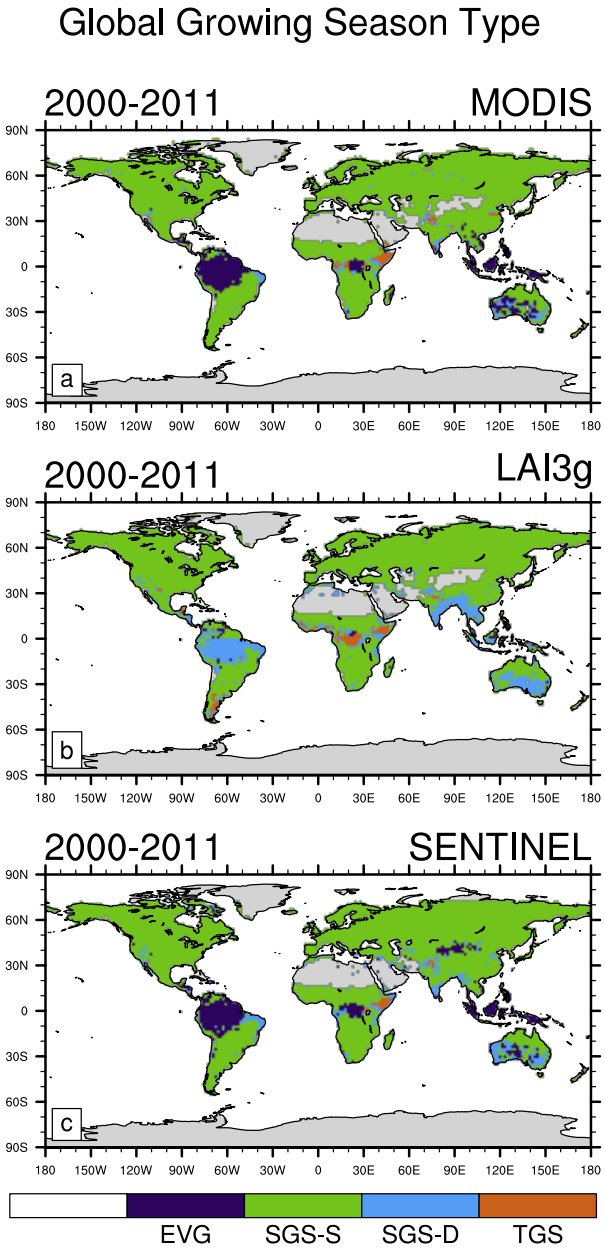

Supplementary Figure 2. Global climatological (averaged over 2000-2011) distribution of the four main growing season modes for (a) MODIS version 6, (b) LAI3g, (c) SENTINEL. Index values: (1, purple) evergreen; (2, green) single season with summer LAI peak; (3, cyan) single growing season with summer dormancy; (4, orange) two growing seasons type.

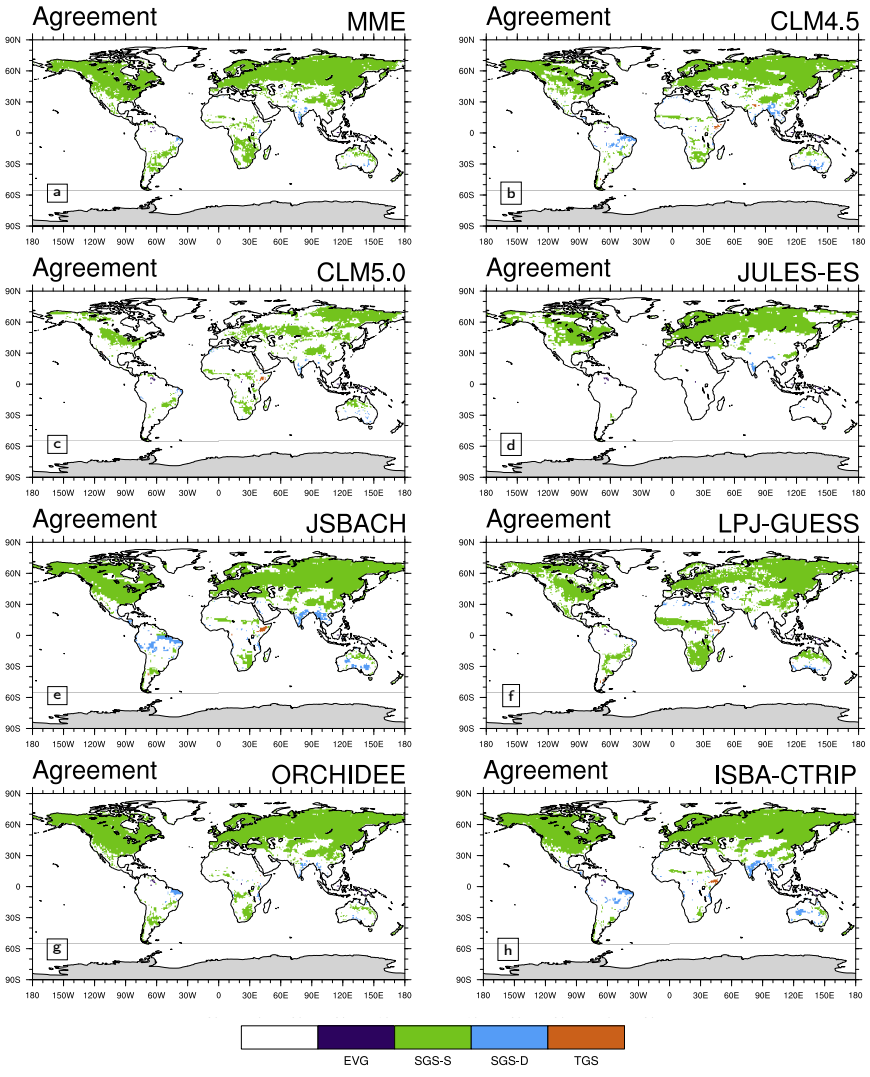

Supplementary Figure 3. Global climatological (averaged over 2000-2011) distribution of the four main growing season modes for (a) Multi-Model Ensemble mean (MME); (b) CLM 4.5; (c) CLM 5.0; (d) JULES-ES; (e) JSBACH; (f) LPJ-GUESS; (g) ORCHIDEE; (h) ISBA-CTRIP. Only the areas characterized by the same type of LAI3g (Supplemetary Figure 2b) are shown. These common areas are called agreement regions. Index values: (1, purple) evergreen; (2, green) single season with summer LAI peak; (3, cyan) single growing season with summer dormancy; (4, orange) two growing seasons type. White regions are for disagreement areas.

Supplementary Table 1. Fraction of land grid-cell in agreement with LAI3g for Multi-Model Ensemble mean (MME) and LSMs in each growing season type. Values are reported in percentage. Colored regions in Supplementary Figure 3.

	CLM 4.5	CLM 5.0	JULES-ES	JSBACH	LPJ-GUESS	ORCHIDEE	ISBA-CTRIP	MME
EVG	56.4	73.7	90.1	21.8	61.2	71.1	72.0	40.2
SGS-S	67.4	44.0	50.4	75.3	76.0	81.3	77.0	78.9
SGS-D	37.4	20.8	5.0	41.1	17.9	20.6	39.6	13.1
TGS	14.0	9.8	0.3	8.3	14.1	3.8	7.1	0.5
Total	58.9	40.3	40.3	64.7	62.4	66.3	66.2	62.6

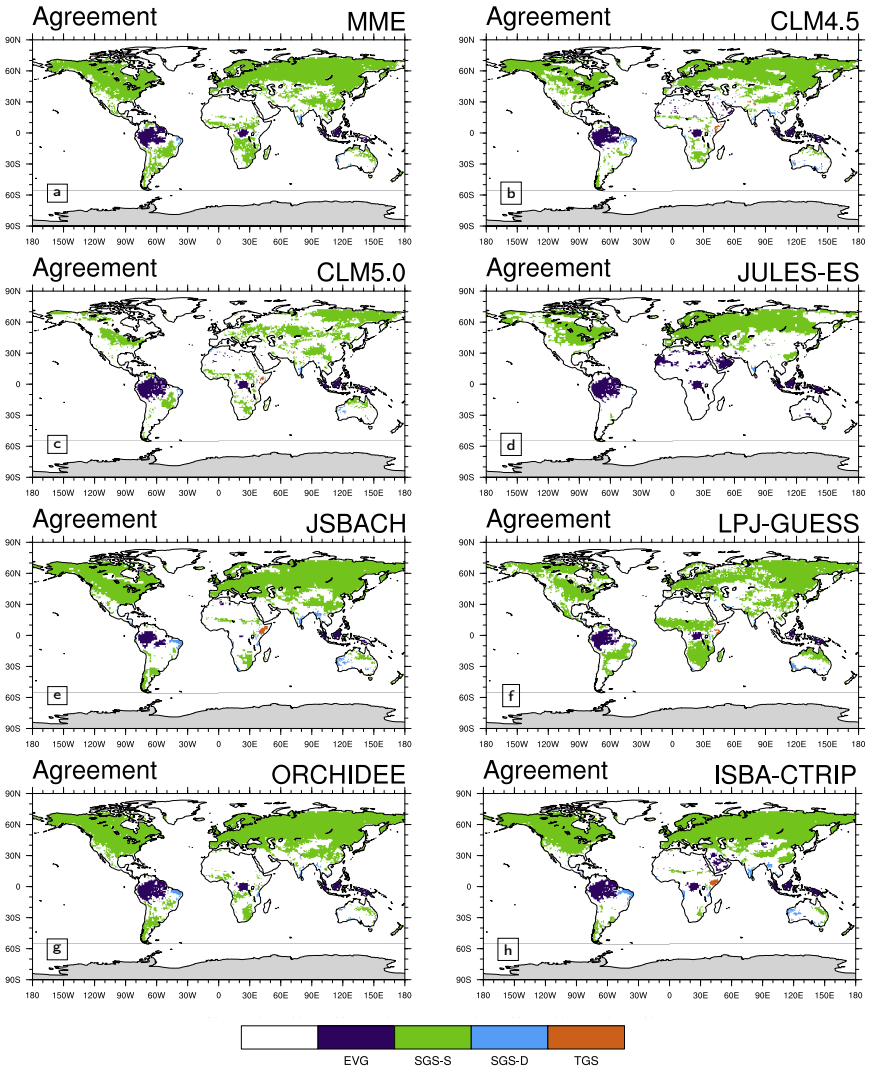

Supplementary Figure 4. Global climatological (averaged over 2000-2011) distribution of the four main growing season modes for (a) Multi-Model Ensemble mean (MME); (b) CLM 4.5; (c) CLM 5.0; (d) JULES-ES; (e) JSBACH; (f) LPJ-GUESS; (g) ORCHIDEE; (h) ISBA-CTRIP. Only the areas characterized by the same type of SENTINEL (Supplemetary Figure 2c) are shown. These common areas are called agreement regions. Index values: (1, purple) evergreen; (2, green) single season with summer LAI peak; (3, cyan) single growing season with summer dormancy; (4, orange) two growing seasons type.

Supplementary Table 2. Fraction of land grid-cell in agreement with SENTINEL for Multi-Model Ensemble mean (MME) and LSMs in each growing season type. Values are reported in percentage. Colored regions in Supplementary Figure 4.

	CLM 4.5	CLM 5.0	JULES-ES	JSBACH	LPJ-GUESS	ORCHIDEE	ISBA-CTRIP	MME
EVG	41.3	46.2	75.4	22.5	32.8	39.2	57.9	29.5
SGS-S	65.3	44.8	48.1	73.0	75.1	79.3	74.1	79.2
SGS-D	42.4	26.5	5.6	43.9	28.8	26.2	47.7	16.6
TGS	21.6	17.8	0.6	14.0	17.8	6.4	13.6	0.7
Total	58.3	42.4	46.5	61.0	63.0	66.3	67.2	63.8

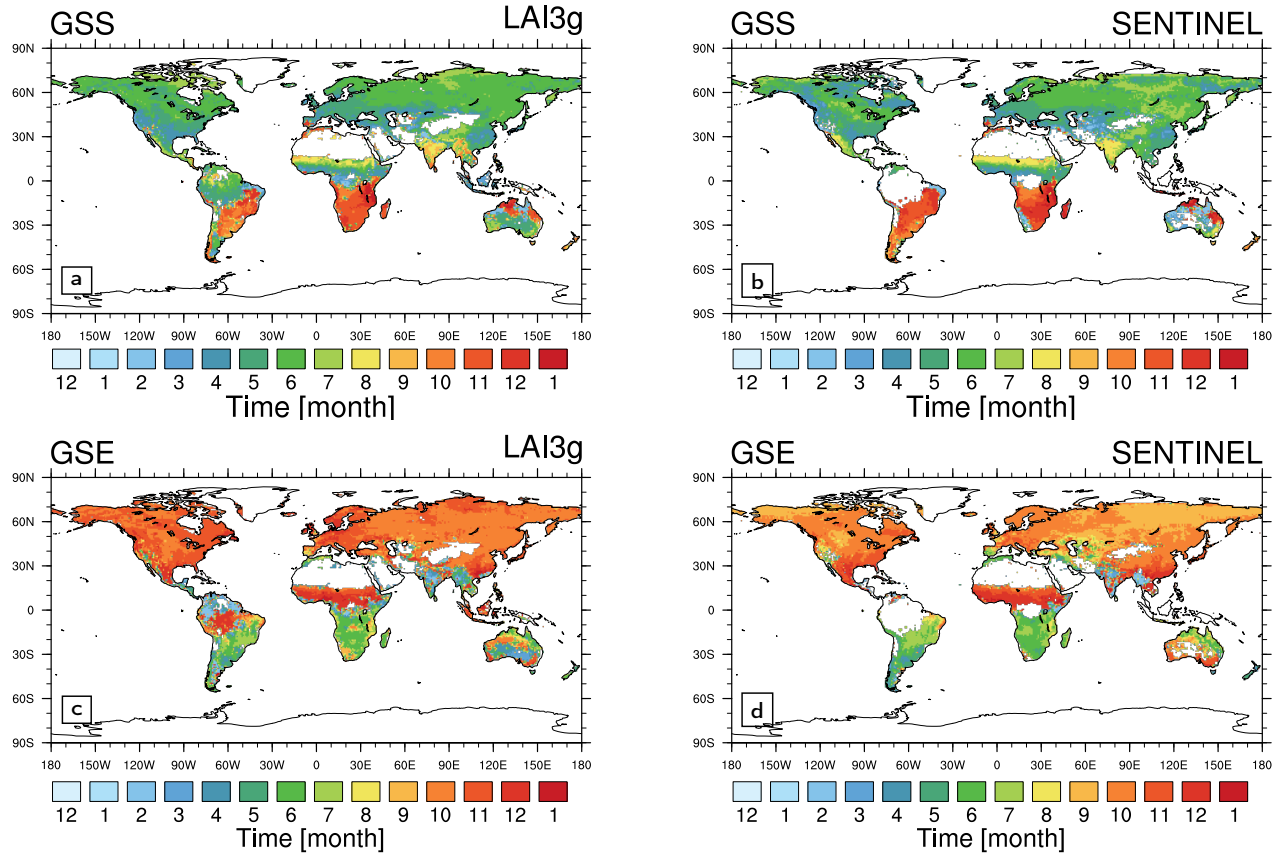

Supplementary Figure 5. Global climatological (averaged over 2000-2011) growing season (a,b) start (GSS) and (c,d) end (GSE) timings for (a,c) LAI3g, and (b,d) SENTINEL.

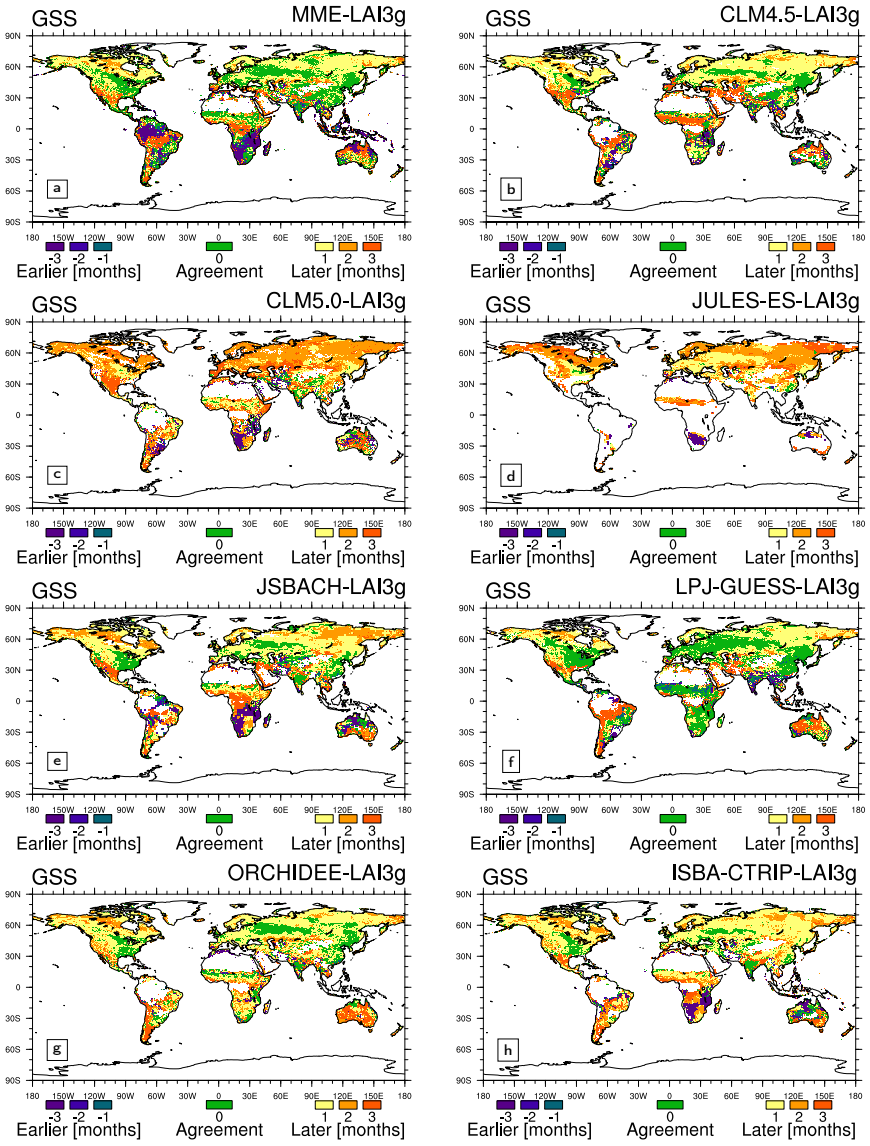

Supplementary Figure 6. Global climatological (averaged over 2000-2011) differences in growing season start (GSS) between (a) Multi-Model Ensemble mean (MME); (b) CLM 4.5; (c) CLM 5.0; (d) JULES-ES; (e) JSBACH; (f) LPJ-GUESS; (g) ORCHIDEE; (h) ISBA-CTRIP and LAI3g (Supplementary Figure 5a). The green regions represent areas of agreement between LAI3g and LSMs. Yellow-red colors correspond to areas where models timings are later compared to LAI3g, while blue-violet colors correspond to areas where models timings are earlier compared to LAI3g. Regions where GSS timings are not computed, such as non-vegetated and evergreen areas, are in white. Note that the GSS in the TGS regions corresponds to the GSS of the first growing season cycle

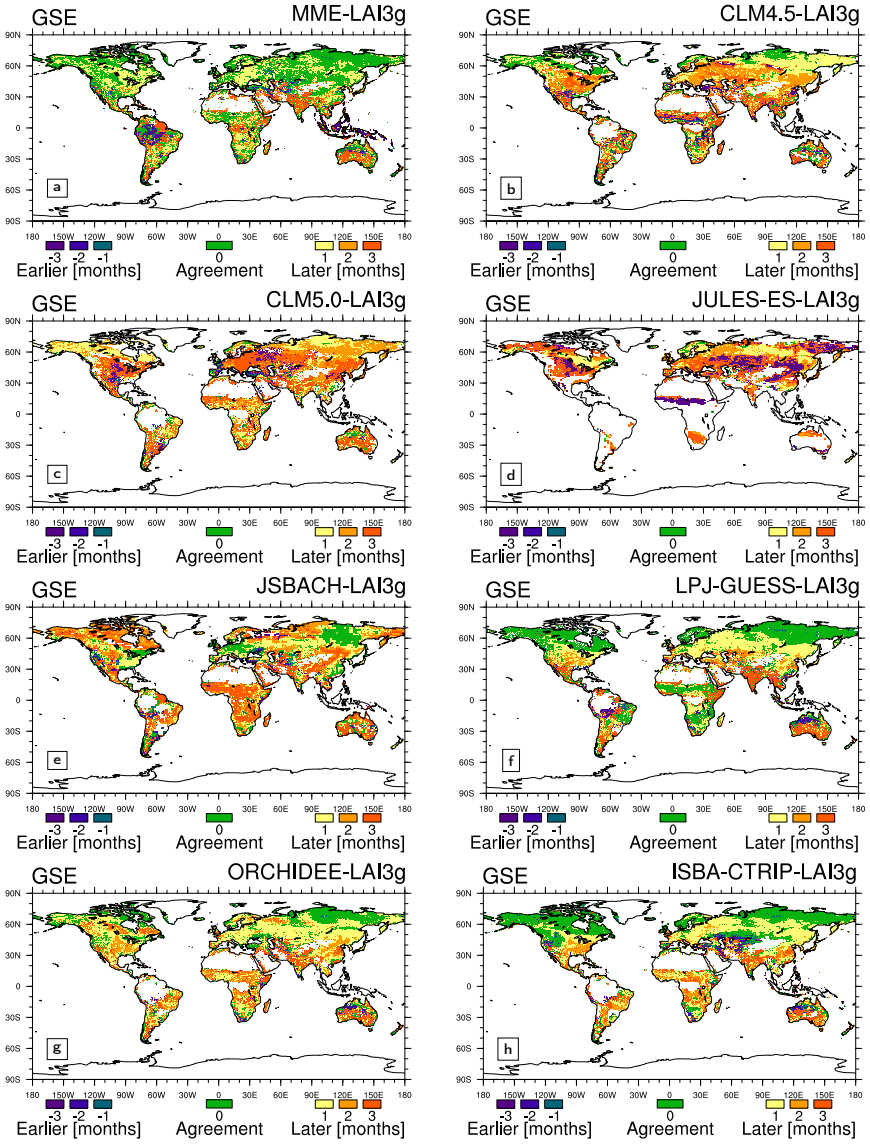

Supplementary Figure 7. As Supplementary Figure 6 but for growing season end (GSE) timings between LAI3g (Supplementary Figure 5c) and Multi-Model Ensemble mean (MME) and LSMs. Note that the GSE in the TGS regions corresponds to the GSE of the second growing season cycle.

Supplementary Table 3. The fraction of land grid-cell in agreement with LAI3g for MODIS, SENTINEL, each land surface model, and multi-model ensemble mean (MME) in growing season start (GSS) and growing season end (GSE) timings. Values are reported in percentages for global, North Hemisphere (NH), and South Hemisphere (SH). Green shaded areas in Supplementary Figures 6 and 7. The last row reports the fraction of land grid-cell in agreement with MODIS for each land surface model in growing season length. The values in brackets give the percentage of global, NH, and SH with a maximum difference of one month.

	MODIS	SENTINEL	CLM 4.5	CLM 5.0	JULES-ES	JSBACH	LPJ-GUESS	ORCHIDEE	ISBA-CTRIP	MME
GSS	34.3	39.4	17.1	5.7	1.9	15.7	25.6	21.7	13.6	16.1
	(66.9)	(71.3)	(52.0)	(20.8)	(16.7)	(50.3)	(57.1)	(58.4)	(55.7)	(38.3)
GSE	40.9	28.7	16.4	5.0	2.3	13.7	22.5	21.6	22.4	23.3
	(72.5)	(66.3)	(38.8)	(22.8)	(11.7)	(36.1)	(54.7)	(54.6)	(58.6)	(43.0)
GSS NH	37.0	43.1	19.0	5.4	2.4	17.9	27.9	24.8	15.5	17.7
	(72.2)	(77.1)	(59.1)	(21.6)	(20.9)	(58.8)	(62.3)	(66.3)	(65.5)	(43.0)
GSE NH	44.8	29.4	17.9	4.2	2.8	15.4	24.8	25.1	26.1	26.3
	(79.2)	(70.8)	(42.1)	(22.5)	(14.6)	(39.9)	(60.3)	(62.0)	(67.0)	(47.7)
GSS SH	24.9	26.5	10.5	6.8	0.4	8.1	18.0	11.2	7.1	10.7
	(48.7)	(51.4)	(27.3)	(18.0)	(2.1)	(20.8)	(39.3)	(31.2)	(21.9)	(22.0)
GSE SH	27.4	26.4	11.4	7.7	0.5	7.8	14.8	9.3	9.7	13.0
	(49.5)	(50.7)	(27.4)	(23.7)	(1.6)	(23.0)	(35.7)	(28.8)	(29.5)	(26.7)
Length	24.6	22.2	16.2	17.2	12.7	16.3	13.5	19.4	18.2	26.1
	(55.8)	(55.8)	(42.6)	(43.5)	(34.1)	(49.4)	(44.6)	(53.0)	(47.0)	(52.3)

Supplementary Table 4. Average difference between LAI3g and MODIS, SENTINEL, each land surface model, and multi-model ensemble mean (MME) in Growing Season Start (GSS) and Growing Season End (GSE) timings. Values are reported in months for global, North Hemisphere (NH) and South Hemisphere (SH). Positive values stand for later timings and negative values correspond to earlier timings.

	MODIS	SENTINEL	CLM 4.5	CLM 5.0	JULES-ES	JSBACH	LPJ-GUESS	ORCHIDEE	ISBA-CTRIP	MME
GSS	-0.25	0.04	0.31	0.54	0.84	0.09	0.22	0.42	0.15	0.33
GSE	0.16	-0.09	-0.08	-0.86	-2.09	-0.03	0.35	0.07	-0.13	-0.27
GSS NH	-0.41	-0.04	0.55	1.07	1.03	0.55	0.06	0.29	0.54	0.54
GSE NH	0.31	-0.13	-0.09	-1.29	-2.36	-0.32	0.47	-0.02	-0.30	-0.45
GSS SH	0.42	0.38	-0.67	-1.73	-2.20	-1.81	0.81	0.97	-1.52	-0.49
GSE SH	-0.46	0.06	-0.07	0.97	2.35	1.16	-0.10	0.44	0.56	0.44

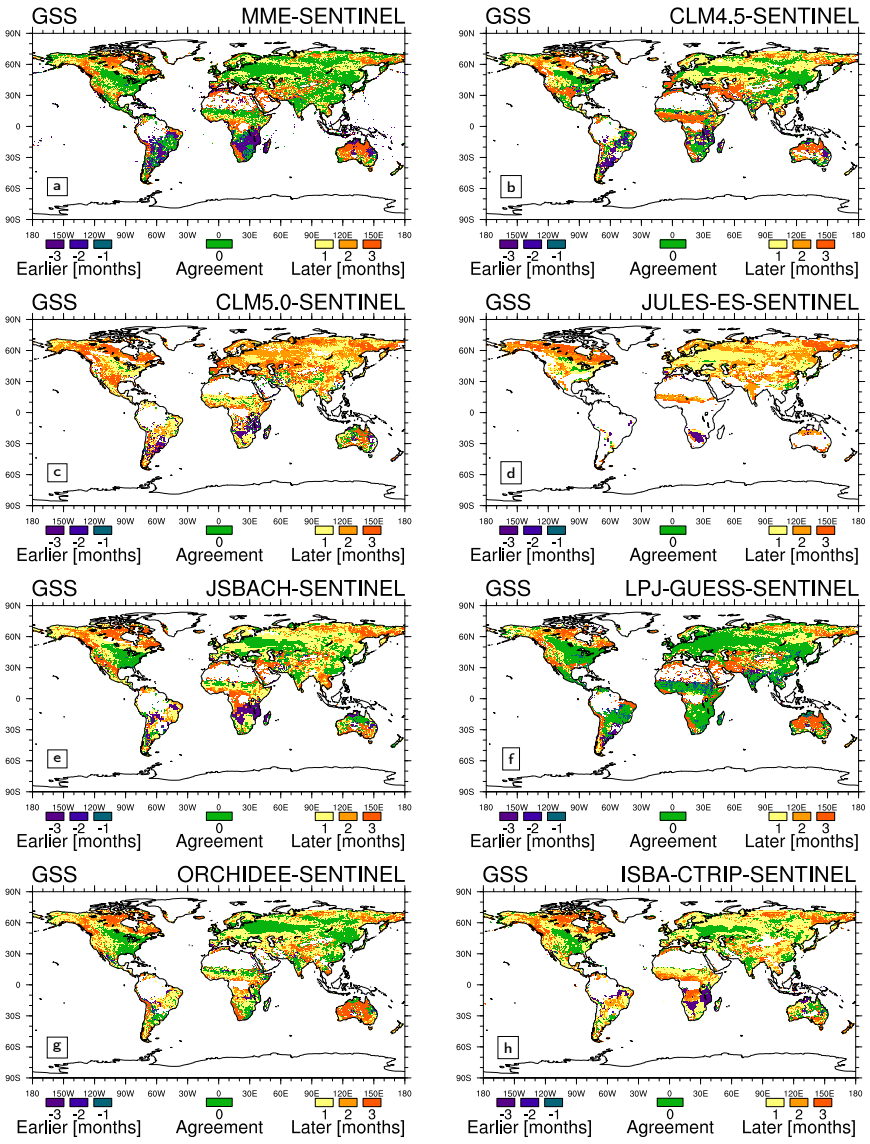

Supplementary Figure 8. As Supplementary Figure 6 but for growing season start (GSS) timings between SENTINEL (Supplementary Figure 5b) and Multi-Model Ensemble mean (MME) and LSMs.

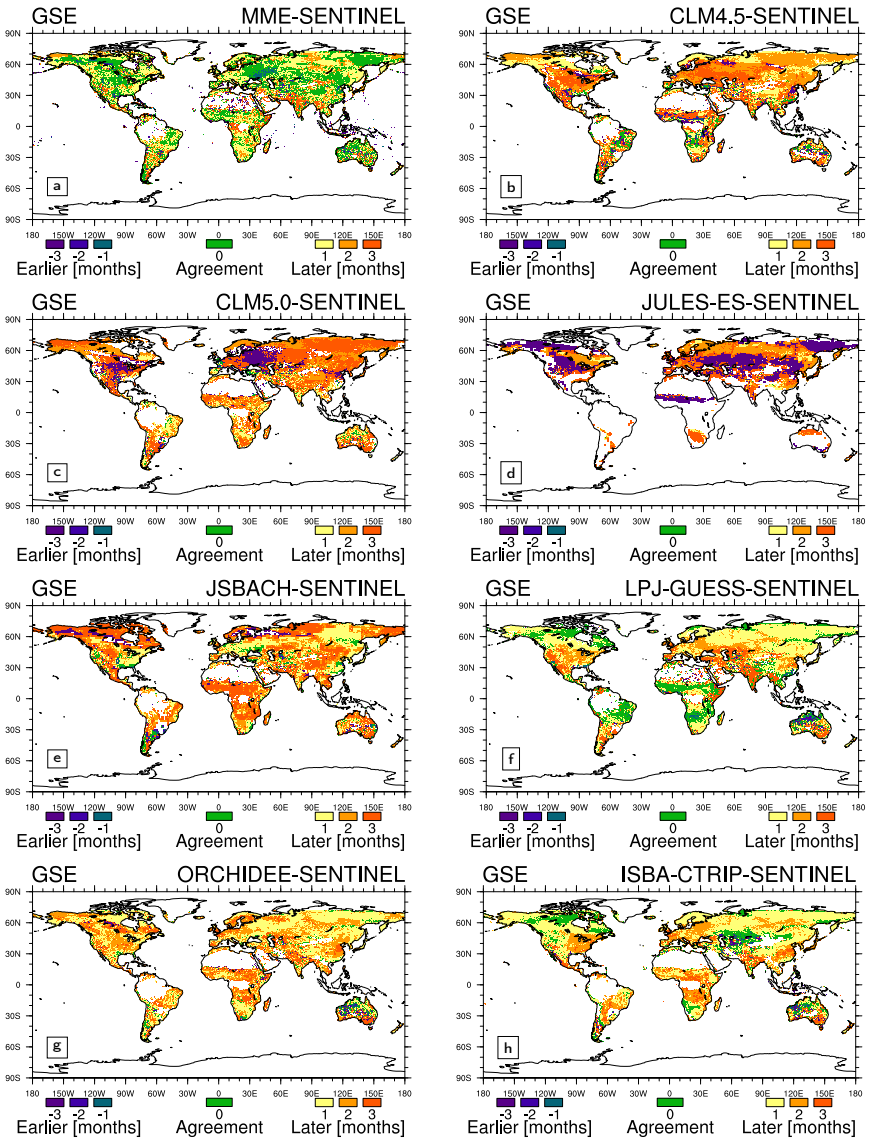

Supplementary Figure 9. As Supplementary Figure 7 but for growing season end (GSE) timings between SENTINEL (Supplementary Figure 5d) and Multi-Model Ensemble mean (MME) and LSMs.

Supplementary Table 5. The fraction of land grid-cell in agreement with SENTINEL for MODIS, LAI3g, each land surface model, and multi-model ensemble mean (MME) in growing season start (GSS) and growing season end (GSE) timings. Values are reported in percentages for global, North Hemisphere (NH), and South Hemisphere (SH). Green shaded areas in Supplementary Figures 8 and 9. The last row reports the fraction of land grid-cell in agreement with MODIS for each land surface model in growing season length. The values in brackets give the percentage of global, NH, and SH with a maximum difference of one month.

	LAI3g	MODIS	CLM 4.5	CLM 5.0	JULES-ES	JSBACH	LPJ-GUESS	ORCHIDEE	ISBA-CTRIP	MME
GSS	42.1	42.2	24.3	7.3	3.2	24.3	28.1	29.5	24.1.	26.0
	(76.2)	(71.6)	(53.0)	(32.1)	(25.8)	(57.2)	(57.5)	(60.5)	(62.2)	(49.6)
GSE	30.3	32.4	7.5	3.2	0.1	5.9	18.2	7.6	16.8.	19.7
	(69.9)	(67.3)	(27.8)	(11.8)	(2.6)	(28.6)	(55.4)	(42.7)	(56.8)	(39.5)
GSS NH	44.4	38.6	26.9	6.7	3.9	26.8	31.3	32.4	26.6	29.3
	(79.4)	(70.6)	(58.1)	(33.1)	(31.3)	(62.9)	(60.3)	(65.3)	(68.2)	(55.9)
GSE NH	29.8	28.5	5.3	2.2	0.1	5.7	17.0	6.6	17.5	20.0
	(72.0)	(65.5)	(26.0)	(7.8)	(2.9)	(30.3)	(54.9)	(44.2)	(60.8)	(39.9)
GSS SH	32.5	56.7	14.1	9.9	0.6	13.9	14.7	17.5	13.7	12.4
	(62.9)	(75.7)	(32.0)	(28.1)	(3.2)	(33.9)	(45.9)	(41.2)	(37.4)	(23.7)
GSE SH	32.0	48.7	16.3	7.3	0.1	6.4	22.9	11.6	13.6	18.5
	(61.4)	(74.8)	(35.5)	(28.0)	(1.2)	(21.6)	(57.2)	(36.8)	(40.4)	(37.6)
Length	23.1	27.7	10.2	13.1	13.4	16.5	12.5	16.0	24.2	22.2
	(58.1)	(52.0)	(32.0)	(38.9)	(36.1)	(45.4)	(42.5)	(49.3)	(56.2)	(46.0)

Supplementary Table 6. Average difference between SENTINEL and LAI3g, MODIS, each land surface model, and multi-model ensemble mean (MME) in Growing Season Start (GSS) and Growing Season End (GSE) timings. Values are reported in month for global, North Hemisphere (NH) and South Hemisphere (SH). Positive values stand for later timings and negative values correspond to earlier timings.

	LAI3g	MODIS	CLM 4.5	CLM 5.0	JULES-ES	JSBACH	LPJ-GUESS	ORCHIDEE	ISBA-CTRIP	MME
GSS	-0.04	-0.30	0.23	0.52	0.79	0.07	0.13	0.35	0.11	0.27
GSE	0.09	0.31	0.03	-0.79	-1.77	0.06	0.44	0.22	0.02	-0.19
GSS NH	0.04	-0.38	0.59	1.09	0.96	0.58	0.09	0.30	0.58	0.60
GSE NH	0.13	0.48	0.05	-1.16	-2.05	-0.16	0.59	0.20	-0.10	-0.35
GSS SH	-0.38	0.01	-1.30	-2.01	-2.06	-2.30	0.31	0.59	-1.97	-1.12
GSE SH	-0.06	-0.39	-0.06	0.84	2.77	1.11	-0.18	0.34	0.56	0.46

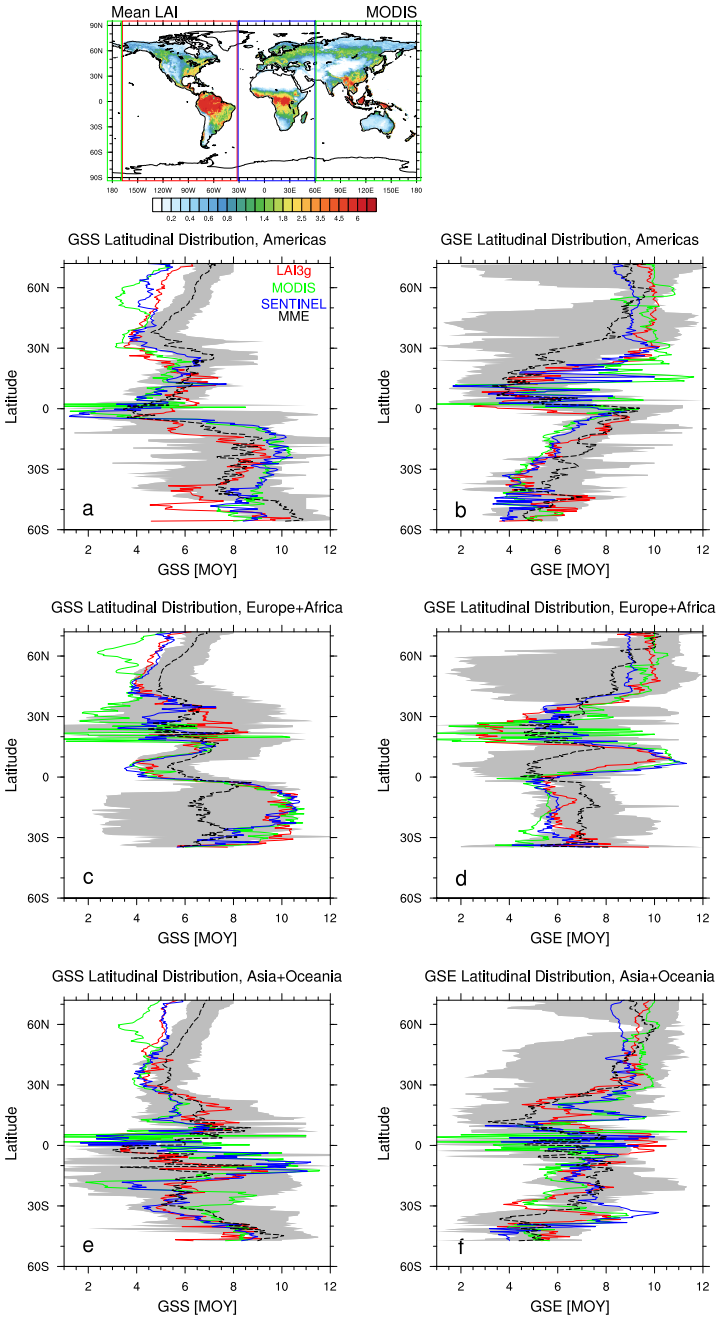

Supplementary Figure 10. Zonal mean (a,c,e) growing season start (GSS) and (b,d,f) growing season end (GSE) timings for LAI3g (red lines), MODIS (green lines), SENTINEL (blue lines), and multi-model ensemble mean (black dashed line). The grey regions show the multi-model ensemble spread. The zonal means are computed over three specific regions: (a,b) Americas (170 – 35°W, red rectangle in the upper map); (c,d) Europe plus Africa (35°W – 60°E, blue rectangle in the upper map); (e,f) Asia plus Oceania (60°E – 170°W, green rectangle in the upper map). Values are reported as months of the year (MOY)

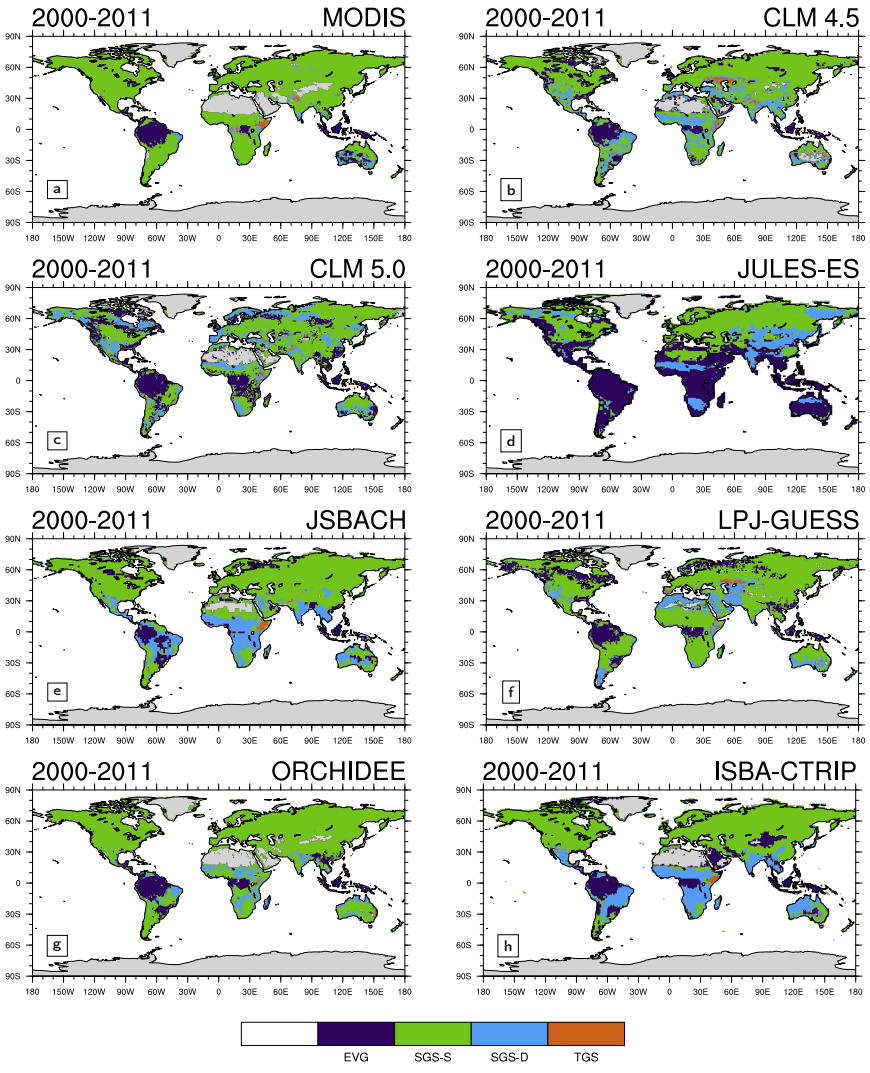

Supplementary Figure 11. Global climatological (averaged over 2000-2011) distribution of the four main growing season modes for (a) MODIS, (b) CLM 4.5; (c) CLM 5.0; (d) JULES-ES; (e) JSBACH; (f) LPJ-GUESS; (g) ORCHIDEE; (h) ISBA-CTRIP. Index values: (1, purple) evergreen; (2, green) single season with summer LAI peak; (3, cyan) single growing season with summer dormancy; (4, orange) two growing seasons type. It is important to keep in mind that evergreen regions are detected as areas where changes in annual LAI cycle are smaller than 25% of the local annual LAI mean value (*Peano et al.*, 2019).

References

Li, W., N. MacBean, P. Ciais, P. Defourny, C. Lamarche, S. Bontemps, R. A. Houghton, and S. Peng (2018), Gross and net land cover changes in the main plant functional types derived from the annual ESA CCI land cover maps (1992–2015), *Earth System Science Data*, *10*, 219–234, https://doi.org/10.5194/essd-10-219-2018

Peano, D., S. Materia, A. Collalti, A. Alessandri, A. Anav, A. Bombelli, and S. Gualdi (2019), Global variability of simulated and observed vegetation growing season, *JGR: Biogeosciences*, *124*, https://doi.org/10.1029/2018JG004881.